



# Fabrication of activated carbon from pomegranate husk by dual consecutive chemical activation for 4-chlorophenol adsorption

Sousan Hadi<sup>1,2</sup> · Ensiyeh Taheri<sup>1,3</sup> · Mohammad Mehdi Amin<sup>1,3</sup> · Ali Fatehizadeh<sup>1,3</sup>  · Eder C. Lima<sup>4</sup>

Received: 23 August 2020 / Accepted: 9 November 2020 / Published online: 17 November 2020  
© Springer-Verlag GmbH Germany, part of Springer Nature 2020

## Abstract

In the present work, the fabrication of activated carbon (AC) from pomegranate husk (PHAC) by dual consecutive activation processes with  $ZnCl_2$  and NaOH as a chemical agent was studied. After that, the synthesized PHAC was used for adsorption of 4-chlorophenol (4CP) as a highly toxic compound for the human health and the environment. Different analytical techniques characterized the synthesized PHAC using  $ZnCl_2/NaOH$ . The isotherms of  $N_2$  adsorption and desorption showed that total pore volume ( $V_{total}$ ) and specific surface area ( $S_{BET}$ ) of PHAC were  $0.404\text{ cm}^3/\text{g}$  and  $811.12\text{ m}^2/\text{g}$ , respectively. The 4CP adsorption by PHAC studies revealed that the highest 4CP removal efficiency was 100% and obtained at 50, 100, and 150 mg/L of 4CP concentration with 2.5 g/L of PHAC. Based on the batch experiments, the highest 4CP removal was achieved at pH 6, 2.5 g/L of PHAC, and contact time of 60 min. The 4CP adsorption data of equilibrium and kinetics were successfully fitted to Langmuir's isotherm and Avrami fractional order.

**Keywords** Adsorption · Activated carbon · Agricultural waste · 4-Chlorophenol

## Introduction

The phenolic compounds (PCs) represent the high toxicity and accumulation potential in the environment and are known as one of the great concern pollutants. The PCs were detected in the effluent wastewater of many industries, such as paper, synthetic rubber, petrochemical units, oil refineries, textile, pharmaceutical industries, and coal gasification sites (Bilgili 2006). The chlorophenols (CPs) belong to a category of PCs and produced with the addition of one to five chlorine atoms

to phenol ring. When CPs contain higher than two chlorine atoms, its structure, it was employed as pesticide agents, and besides, the 4-chlorophenols (4CP) are classified as antiseptics. During water disinfection, the 4CPs are produced as disinfection by-products when water containing PCs and also in paper production industries are created when chlorine is used for wood pulp bleaching (Bilgili et al. 2012).

For the removal of PCs from wastewater, several technologies, including photocatalytic processes, advanced oxidation processes, biological and membrane filtration, and adsorption processes, have been employed (Hadi et al. 2020). The activated carbons (ACs) are extensively applied for PCs adsorption from liquid and gaseous fluids. For ACs preparation, the various precursors including coal, peat, and lignite as a raw carbon resource and also sawdust, wood, bagasse, and agricultural by-products as biomass resources have been used (Gratuito et al. 2008). Generally, the ACs production process is divided into two distinct steps: first, carbonization of raw materials under an inert atmosphere ( $N_2$  or argon gas) and, second, the carbonized product activation. The chemical activation, physical activation, or combination were used for the activation process (Latinwo et al. 2019). Compared with physical activation, the main advantages of chemical activation are a lower temperature of activation, the higher yield, shorter activation time, and higher porosity development. The

Responsible Editor: Tito Roberto Cadaval Jr

✉ Ali Fatehizadeh  
a.fatehizadeh@hlth.mui.ac.ir

<sup>1</sup> Department of Environmental Health Engineering, School of Health, Isfahan University of Medical Sciences, Isfahan, Iran

<sup>2</sup> Student Research Committee, School of Health, Isfahan University of Medical Sciences, Isfahan, Iran

<sup>3</sup> Environment Research Center, Research Institute for Primordial Prevention of Non-Communicable Disease, Isfahan University of Medical Sciences, Isfahan, Iran

<sup>4</sup> Institute of Chemistry, Federal University of Rio Grande do Sul (UFRGS), Av. Bento Gonçalves 9500, Postal Box 15003, Porto Alegre, RS 91501-970, Brazil

required additional washing stage and application of expensive activating agents (KOH and NaOH vs.  $\text{CO}_2$  and  $\text{H}_2\text{O}$ ) are the disadvantages of chemical activation (Maciá-Agulló et al. 2004). During the carbonization of carbonaceous material, the volatile components of the biomass are lost during the pyrolysis, originating a solid char. In this step, there is a formation of aromatic rings that are condensed irregularly. The obtained carbonized product (char) showed low adsorption capacity due to the low surface area, and it must be activated to increase absorption capacity (Wigmans 1989).

The present work aimed to investigate the removal efficiency of 4CP from aqueous solutions fabricated ACs from pomegranate husk (PHAC) by dual consecutive chemical activation. The XRD, EDS, SEM, FTIR, and BET analysis were employed to determine the physicochemical properties of PHAC. Besides, to find the optimum condition of 4CP removal from aqueous effluents, we conducted a comprehensive batch experiment using different experimental conditions including solution pH, contact time, PHAC dose, initial 4CP concentration, ionic strength, and temperature. To demonstrate the 4CP adsorption mechanisms and dynamics, frequent adsorption isotherm models such as Langmuir, Freundlich, and Liu and kinetic models, including pseudo-first-order, pseudo-second-order, Elovich, and Avrami fractional order, were employed.

## Materials and methods

### Materials and devices

In the present study, the analytical grade of 4CP (micropollutant),  $\text{ZnCl}_2$ , and NaOH was purchased from Merck Co (Darmstadt, Germany). For solutions preparing and material rinsing, the distilled water was used. A 4CP stock solution with a concentration of 1000 mg/L was made by the dissolution of  $\text{C}_6\text{H}_5\text{ClO}$  (1.0 g) in dual deionized water (1000 mL) with some heating. The other required solutions were prepared from the 4CP stock solution. The initial pH of each test solution was adjusted with HCl and/or NaOH (0.1 M).

**Table 1** Elemental composition of PH and PHAC

Element	Material type	
	Raw PH	PHAC
C (%)	46.52	62.05
H (%)	2.73	0.83
N (%)	0.72	1.32
S (%)	0.15	0.12

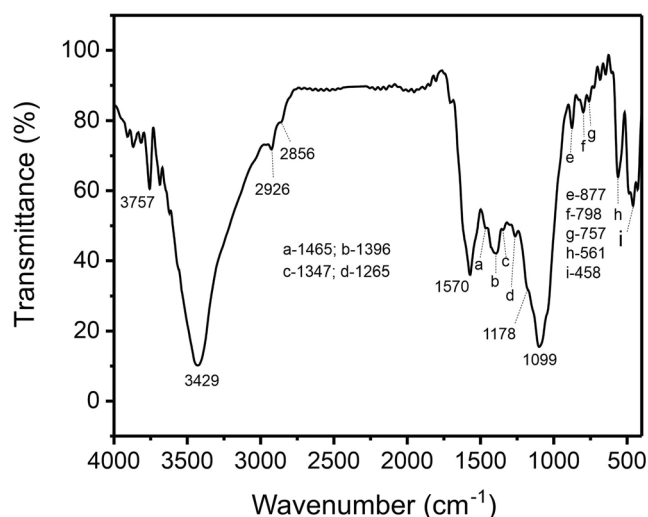


**Fig. 1** FTIR spectrum of PHAC

### PHAC fabrication

The raw PHs were collected from the local fruit shops (Isfahan, Iran) and washed with deionized water many times to remove any impurities and dried at 105 °C for 12 h. The dried PHs were mechanically ground and sieved by standard mech No. 16 (1.18 mm). With the application of activation agents including  $\text{ZnCl}_2$  and NaOH, ACs were obtained in two subsequent chemical activation stages.

In the first chemical activation, 50 g of raw PH was blended with 100 mL of the  $\text{ZnCl}_2$  activating agent (3 M) for 2 h and thoroughly washed with HCl solution (0.1 M), rinsed with deionized water, and dried at 105 °C. After that, the thermal carbonization, including 550 °C for 2 h under 100 mL/min  $\text{N}_2$  purging, was applied and then treated with HCl (6 mol/L) to inorganic components leaching from the carbonized material and rinsed with deionized water and dried at 105 °C (Fatehizadeh et al. 2019).

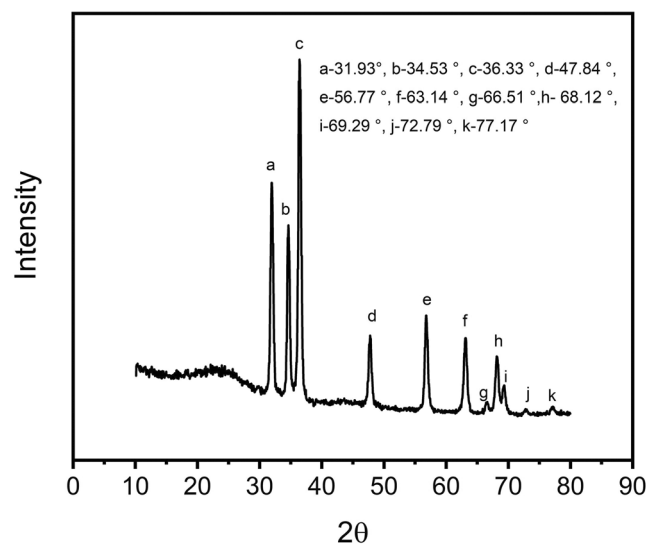


**Fig. 2** XRD pattern of PHAC

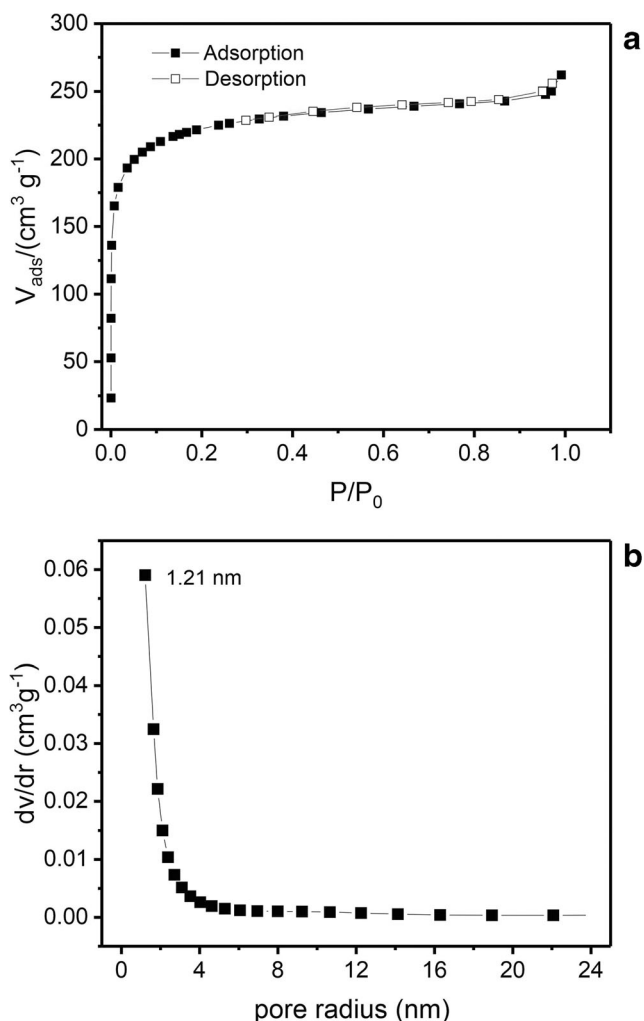


**Fig. 3** Textural characteristics of PHAC, **a** isotherms of N<sub>2</sub> adsorption and desorption, **b** pore size distribution curve

After the first activation step, the adsorbents obtained were subjected to the NaOH second activation stage same as a first stage with another chemical activation agent and followed by thermal carbonization and acid leaching. Finally, all obtained PHACs were thoroughly washed many times with deionized water until they attained the pH of 6 for PHAC, dried for 2 h at 105 °C, and stored in a glass bottle until used.

### Experiments

The experiment of batch 4CP adsorptions was conducted in the Erlenmeyer flask (150 mL) containing 50 mL of 4CP solution with a gas-tight cap in triplicate. The removal efficiency of 4CP with PHAC was comprehensively investigated under various conditions of batch experiments including solution pH (3–9), contact time (5–120 min), a dose of PHAC (0.5 to 2.5 g/L), initial 4CP concentration (20–150 mg/L), ionic strength (0.01–0.3 mol/L), and adsorption temperature (283–313 K). The test solutions were agitated at 200 rpm/min

to ensure complete contact between 4CP molecules and PHAC. After experiments conduction, the test solutions were filtered and subjected to 4CP concentration analysis.

### Determination of PHAC characterizations and analysis

After synthesizing PHACs, its physical properties were determined by XRD, EDS, FESEM, BET, Mapping, and FTIR analyses. In order to adjudge the pH value at the point of zero charge ( $pH_{pZC}$ ), the drift method was employed (Kosmulski 2009). The 4CP concentration was determined by a colorimetric method as 100  $\mu$ L of 4-aminoantipyrine and  $K_3Fe(CN)_6$  solutions were added to 800  $\mu$ L of sample and after 5 min reaction time, the colorfully created. After that, the aliquot absorbance was measured at wavelength 510 nm using a UV-Vis spectrophotometer (UNICO 2150-UV, China) (Hadi et al. 2020). The solution pH was measured with a pH meter (CG 824 SCHOTT). According to Eqs. 1 and 2, the adsorption efficiency of 4CP and adsorption capacity were computed.

$$R = \frac{C_0 - C_f}{C_0} 100 \tag{1}$$

$$q_e = \frac{C_0 - C_f}{m} V \tag{2}$$

where  $R$  and  $q_e$  are 4CP removal efficiency (%) and adsorption capacity (mg/g), respectively;  $C_0$  and  $C_f$  are the 4CP concentrations in solution at the initial and final of the batch adsorption (mg/L), respectively;  $m$  is the adsorbent mass (g); and  $V$  is the sorbing solution volume (L).

## Results and discussion

### Characterization of PHAC

#### Elemental composition and functional group of PHAC

The elemental compositions of raw PH and PHAC are summarized in Table 1.

As can be seen, the carbon content of raw PH is lower than the PHAC. The raw PH contained 46.52% of carbon, 0.72% of nitrogen, 2.73% of hydrogen, and 0.15% of sulfur. Nevertheless, the PHAC fabrication with dual consecutive chemical activation leads to increasing the PHAC carbon content to 62.05%. In contrast, the hydrogen content dropped to 0.83%, following the same trend that was described by Umpierrez et al. (2018) who studied the preparation of ACs from tucumã (TUC) by microwave heating and demonstrated that the TUC carbon contents improved from 48.8 to 81.5% when converted to AC.

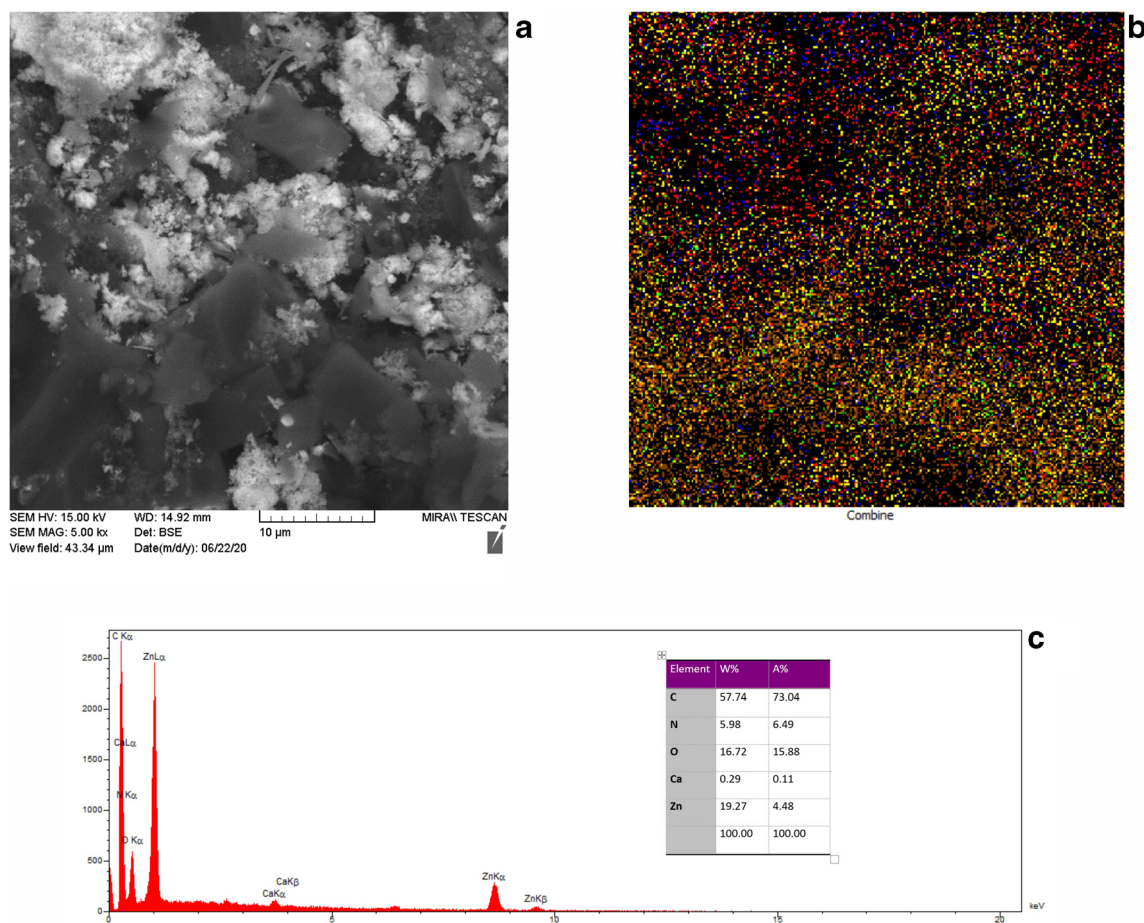


**Fig. 4** FESEM micrographs of PHAC (a), mapping analysis (b), EDX result (c)

Furthermore, the FTIR test was employed to determine the functional groups of PHAC. Figure 1 illustrates the obtained spectrum of FTIR for PHAC.

The band at 458 and 561  $\text{cm}^{-1}$  may be allocated to Zn-O bands (Babu et al. 2013). The bands at 757, 798, and 877  $\text{cm}^{-1}$  are related to aromatic out of the plan -CH bending (Ribas et al. 2014). The intense broadband at 1099  $\text{cm}^{-1}$  is assignable to the asymmetric C-O-C ether or O-C-C of an aromatic ester. The shoulder at 1178  $\text{cm}^{-1}$  could be appointed to C-O of phenol. The vibrations detected at 1465, 1396, and 1347  $\text{cm}^{-1}$  are established to the aromatic ring modes (Gupta and Nayak 2012). The band at 1570  $\text{cm}^{-1}$  is assignable to the asymmetric carboxylate band (Lima et al. 2019). The bond of 2926 and 2856  $\text{cm}^{-1}$  is related to asymmetric stretching of C-H groups. The broadband at 3429  $\text{cm}^{-1}$  is assigned to OH stretching (Sajjadi et al. 2019).

#### X-ray diffraction and BET of PHAC

To determine the structural characteristics of PHAC, the XRD was employed (Fig. 2).

It can be observed that PHAC has sharp distinguishing diffraction peaks at  $2\theta = 31.93^\circ, 34.53^\circ, 36.33^\circ, 47.84^\circ, 56.77^\circ, 63.14^\circ, 66.51^\circ, 68.12^\circ, 69.29^\circ, 72.79^\circ,$  and  $77.17^\circ$ , respectively, corresponding to zinc oxide (JCPDS file no. 01-079-0205) and related to the application of activating agents during PHAC production.

The BET analysis according to the adsorption and desorption isotherms of  $\text{N}_2$  gas is the practical method for evaluating the total pore volume ( $V_{total}$ ), specific surface area ( $S_{BET}$ ), pore size, and monolayer volume of adsorbent. The adsorption and desorption isotherms of  $\text{N}_2$  gas and distribution of pore size curves based on the DFT method are illustrated in Fig. 3.

Therefore, the main properties of PHAC, including  $V_{total}$ ,  $S_{BET}$ , and average pore diameter, were 0.404  $\text{cm}^3/\text{g}$ , 811.12  $\text{m}^2/\text{g}$ , and 1.21 nm, respectively. The better characteristics of AC were stated by Sajjadi et al. (2019). They reported that the  $V_{total}$ ,  $S_{BET}$ , and pore diameter of  $\text{NH}_4\text{NO}_3$  and NaOH-activated carbon from pistachio wood were 0.994  $\text{cm}^3/\text{g}$ , 1884  $\text{m}^2/\text{g}$ , and 2.11 nm, respectively. However, in contrast, Ribas et al. (2014) synthesized acidified AC from a cocoa shell (ACC-1) and reported that the  $V_{total}$ ,  $S_{BET}$ , and pore diameter



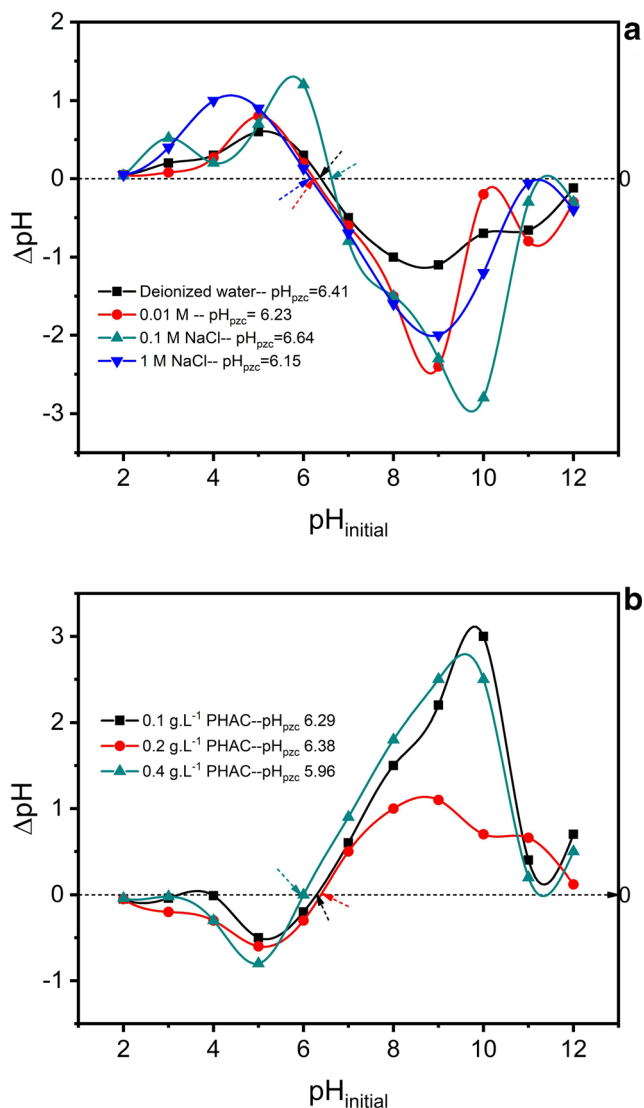


**Fig. 5** Effects of various operation conditions on the  $pH_{pzc}$  of PHAC, **a** NaCl concentration, **b** PHAC dose

of ACC-1 were respectively 0.459 cm<sup>3</sup>/g, 522 m<sup>2</sup>/g, and 5.23 nm.

**EDS map and PHAC morphology**

The morphology of PHAC was exhibited in Fig. 4a. The carbon material presents some rugosity at the magnification of 5000-fold. The results of the mapping analysis illustrated in Fig. 4b also confirm that the distribution of elements at the PHAC surface is performed uniformly. According to EDS analysis (Fig. 4c) of the PHAC, the peaks of C, N, O, Ca, and Zn could be seen which indicated that the chemical composition of PHAC includes carbon (57.74%), nitrogen (5.98%), oxygen (16.72%), calcium (0.29%), and zinc (19.27%) which once again suggesting the synthesis of PHAC.

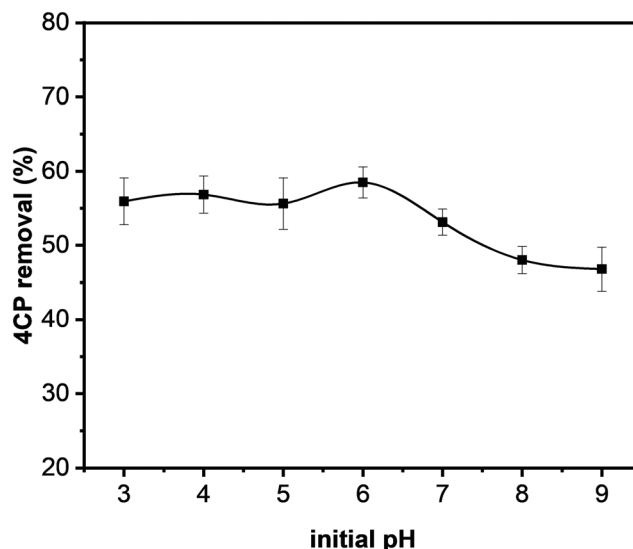


**Fig. 6** Variation of 4CP adsorption by changing solution pH (4CP concentration, 20 mg/L; AC dose, 0.4 mg/L; temperature, 20 °C; and contact time, 60 min)

**Point of zero charge**

The isoelectric point (IEP) or  $pH_{pzc}$  was used to demonstrate the electrical surface state of adsorbent, especially AC. The series of solutions using NaCl as background electrolyte was prepared with initial pH value ( $pH_i$ ) from  $pH\ 2.0 \pm 0.2$  to  $11 \pm 0.2$  to find the  $pH_{ZPC}$ . With adding desire PHAC mass into each solution, the containers were immediately sealed, and the suspensions were shaken for 48 h at 150 rpm. After that, the final pH value ( $pH_f$ ) of each solution was documented, and the

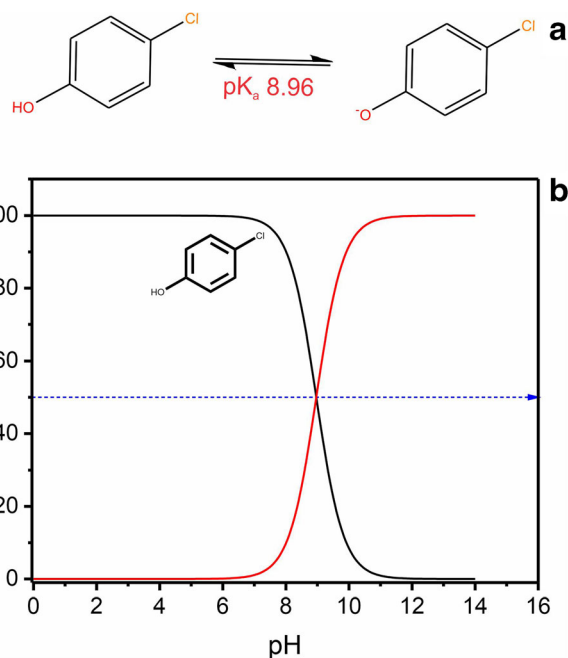


**Fig. 7** (a)  $pK_a$  and (b) distribution of the species of 4CP in the function of pH

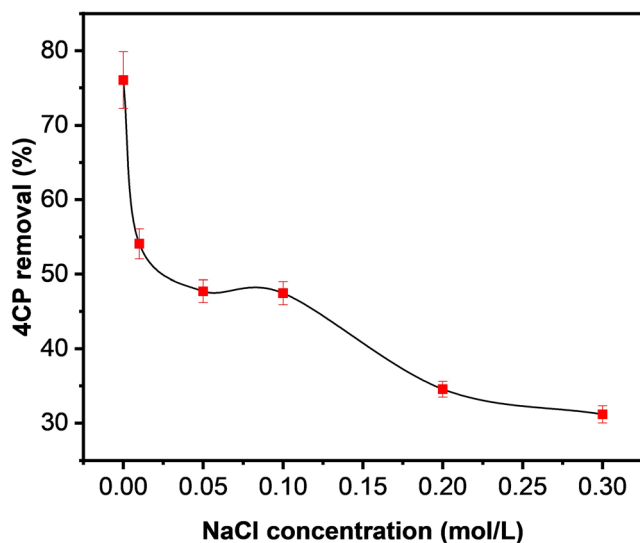


**Fig. 8** Influence of NaCl concentration on 4CP adsorption by PHAC (4CP concentration, 20 mg/L; PHAC dose, 0.4 mg/L; solution pH, 6; temperature, 20 °C; and contact time, 60 min)

$\Delta$ pH was plotted against  $pH_i$ . Figure 5 illustrates the effect of influencing parameters on  $pH_{pzc}$  of PHAC, including the concentration of background electrolyte and PHAC dose.

From Fig. 5, the  $pH_{pzc}$  was determined from the point of intersection of the  $\Delta$ pH ( $pH_{final} - pH_{initial}$ ) with  $pH_{initial}$ . As can be seen, the  $pH_{pzc}$  of PHAC ranged from 6.15 to 6.41 in a medium ranging from deionized water to 1 M NaCl (Fig. 5a). When the PHAC dose varied from 0.1 to 0.4  $g \cdot L^{-1}$ , the  $pH_{pzc}$  ranged from 5.96 to 6.38.

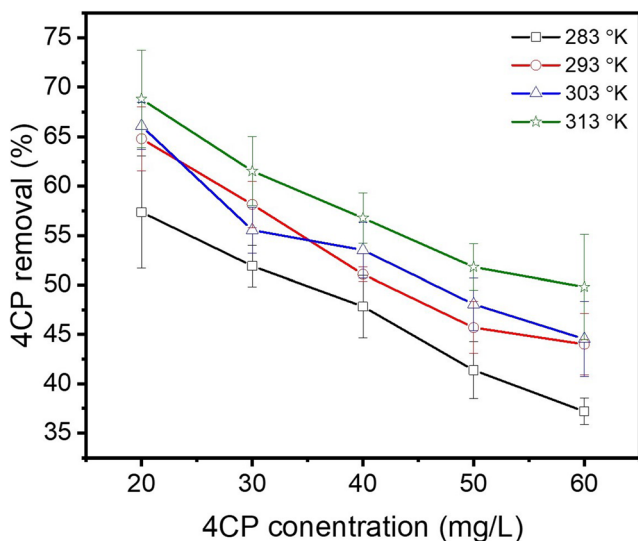


**Fig. 9** Variation of 4CP adsorption as a function of temperature (4CP concentration, 20–60 mg/L; PHAC dose, 0.4 mg/L; solution pH, 6; and contact time, 60 min)

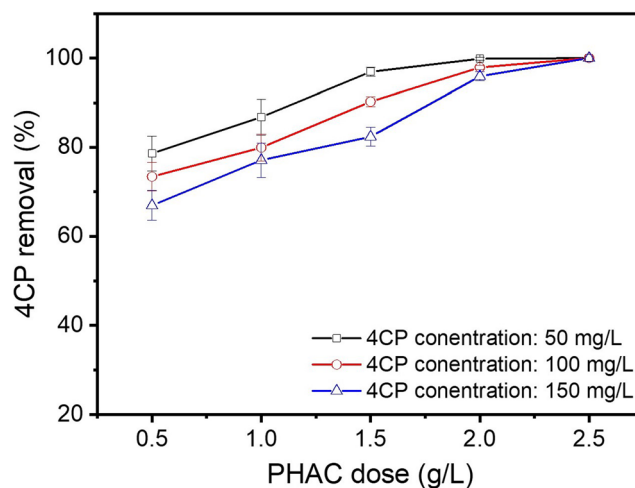


**Fig. 10** Influence of PHAC dose on 4CP adsorption (4CP concentration, 50–150 mg/L; solution pH, 6; temperature, 20 °C; and contact time, 60 min)

## Effect of critical parameters on 4CP adsorption

### Effect of solution pH

The 4CP adsorption by PHAC under different solution pH (3–9) was examined at 20 mg/L of 4CP concentration and shown in Fig. 6.

As illustrated in Fig. 6, the removal efficiency of 4CP improved from  $55.9 \pm 3.2$  to  $58.5 \pm 2.1\%$  with ascending solution pH from 3 to 6. After that, the 4CP removal efficiency reduced as the hydrogen ion concentration increased and reached  $46.8 \pm 3.1\%$  at a solution pH of 9.

It was realized that the 4CP removal by PHAC was extremely dependent on the solution pH, which affected the PHAC surface charge and the 4CP ionization degree. This behavior agrees with the  $pK_a$  value of the 4CP ( $pK_a$  8.96). At pH 6.0, 99.89% of 4CP is presented in the unprotonated specie (Fig. 7) and 0.11% is presented in the anionic specie. Considering that  $pH_{pzc}$  of the adsorbent is 5.96–6.41, at pH values higher than this interval, the surface of the adsorbent becomes with a superficial negative charge. At pH 9.0, 47.91% of 4CP is presented in the undissociated form and 52.09% as dissociate form. Therefore, the dissociate form that is an anion is repulsed from the adsorbent surface (at pH 9), decreasing the percentage of removal considerably.

Besides the charge attraction ( $pH \leq 6$ ) and repulsion ( $pH \geq 6.5$ ) mechanism, hydrogen bonding also plays a role in the mechanism of adsorption. The interactions of OH groups of 4CP with the oxygen present on the carbon surface are also quite probable (Srivastava et al. 1997). The  $\pi$ - $\pi$  interactions

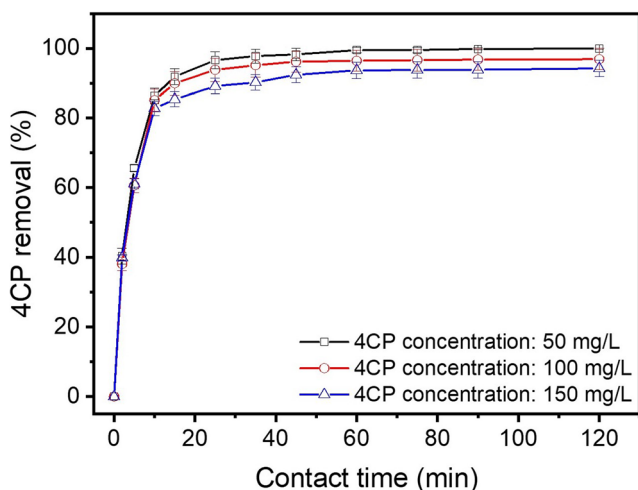


**Fig. 11** Influence of contact time on 4CP adsorption by PHAC (4CP concentration, 50, 100, and 150 mg/L; PHAC dose, 2.0 g/L; solution pH, 6.0; and temperature, 20 °C)

also play a role in the adsorption of 4CP ( $\pi$  bonds of 4CP and  $\pi$  bonds of activated carbon).

**Effect of ionic strength**

Both natural water and industrial wastewater usually contain dissolved salts, which may interfere with the pollutant’s uptake of the adsorbents. The adsorption experiments were performed by the addition of different concentrations of NaCl to evaluate the influence of ionic strength on the 4CP adsorption (Fig. 8).

As illustrated in Fig. 8, with increasing the NaCl concentration from distilled water to 0.3 mol/L, the significant decrease in the removal of 4CP was observed. The inner and outer spheres are two surface complexes that can form along with the adsorption process. The covalent bonds are the dominant chemical link between adsorbed molecules or ions and the adsorbent surface functional groups in the inner sphere surface complexes, and during the outer sphere surface complexes, no covalent bonds form. The ionic strength in sensitivity and adsorption decreasing with ionic strength increasing has been taken as an indication of an inner and outer sphere surface complex, respectively (Wang et al. 2010). Based on the mentioned above, the 4CP adsorption by PHAC in the

present work was followed by the formation of outer sphere complexes.

Furthermore, other interactions, including hydrogen bonding, electrostatic attraction, or hydrophobic attraction, are involved in the adsorption process (Chen and Wang 2007). The inorganic salts (e.g., NaCl, KCl, CaCl<sub>2</sub>, MgCl<sub>2</sub>) in the solution can change the strength of electrostatic interactions of the adsorbent-adsorbate (Kuśmierk et al. 2020). Theoretically, the solution salinity increasing resulted in adsorption capacity declining as the adsorbent surface and adsorbate ions have attractive electrostatic forces. Conversely, the ionic strength increasing leads to improving the adsorption efficiency when the electrostatic attraction is repulsive (Al-Degs et al. 2008). Chen and Wang (2007) found that when adsorption efficiency depends on the ionic strength due to the formation of outer sphere complexes, the interactions of negative charge of adsorbent surface and metal ions lead to cation exchange at sorption sites. Therefore, the increasing concentration of Na<sup>+</sup> and Cl<sup>-</sup> in solution presumably attributed to enhancing the competition with 4CP for the PHAC sorption sites, thus reducing the 4CP adsorption efficiency.

**Effect of temperature**

The 4CP batch adsorption experiments were carried out at different adsorption temperatures ranging from 283 to 313 K at different initial 4CP concentrations and constant PHAC dose (0.4 g/L) and pH of 6, and obtained results are shown in Fig. 9.

It can be seen from Fig. 9, with increasing adsorption temperature, at a particular concentration of 4CP, the 4CP removal percent increased too. The 4CP adsorption increased from 57.36 to 68.81% (20 mg/L of 4CP), 51.91 to 61.52% (30 mg/L of 4CP), 47.82 to 56.76% (40 mg/L of 4CP), 41.37 to 51.80% (50 mg/L of 4CP), and 37.20 to 49.79% (60 mg/L of 4CP) with the climbing of the adsorption temperature from 283 to 313 K. The main effects of temperature on the adsorption process include (i) the solution viscosity decreasing and enhancing the diffusion rate of sorbate within adsorbate pores and (ii) internal bonds breaking of sorbent active surface sites and generating the additional sorption sites (Boudrahem et al. 2009). The results indicated that the adsorption of 4CP adsorbed by PHAC is favored with the increase of the temperature. Shaarani and Hameed (2011) reported similar results and described that the 2,4-dichlorophenol (2,4DCF) adsorption by ammonia-modified AC is gradually improved with adsorption temperature ascending from 30 to 50 °C.

**Influence of AC dose**

The influence of the dose of PHAC on adsorption efficiency of 4CP was investigated by changing the PHAC dose ranging from 0.5 to 2.5 g/L. Figure 10 shows the 4CP removal

**Table 2** Adsorption kinetic models

Kinetic model	Equation
Pseudo-first order	$q_t = q_e [1 - \exp(-k_f t)]$ (3)
Pseudo-second order	$q_t = \frac{k_s q_e^2 t}{1 + (q_e k_s t)}$ (4)
Elovich	$q_t = \frac{1}{\beta} \ln(\alpha \beta) + \frac{1}{\beta} \ln(t)$ (5)
Avrami fractional order	$q_t = q_e [1 - \exp[-(k_{AV} t)^{n_{AV}}]]$ (6)

**Table 3** Values of kinetic parameters and fitting coefficients for 4CP adsorption

Kinetic model	Constant parameter	Initial 4CP concentration (mg/L)		
		50	100	150
Pseudo-first order	$q_e$	24.56 ± 0.19	47.88 ± 0.36	68.93 ± 0.74
	$k_f$	0.23 ± 0.01	0.217 ± 0.009	0.24 ± 0.01
	$R^2_{adj}$	0.996	0.995	0.991
	Reduced chi-square	0.28	0.95	4.21
Pseudo-second order	$q_e$	26.18 ± 0.29	51.10 ± 0.78	73.42 ± 0.80
	$k_S$	0.014 ± 0.001	0.007 ± 0.001	0.0051 ± 0.0010
	$R^2_{adj}$	0.993	0.988	0.994
	Reduced chi-square	0.40	2.65	2.95
Elovich	$\alpha$	100.64 ± 8.6	166.3 ± 14.4	323.67 ± 27.09
	$\beta$	0.30 ± 0.04	0.15 ± 0.02	0.11 ± 0.02
	$R^2_{adj}$	0.934	0.925	0.942
	Reduced chi-square	4.03	17.69	27.83
Avrami fractionary	$q_e$	24.78 ± 0.09	48.17 ± 0.28	69.76 ± 0.54
	$k_{AV}$	0.225 ± 0.005	0.216 ± 0.007	0.23 ± 0.01
	$n_{AV}$	0.82 ± 0.02	0.86 ± 0.04	0.77 ± 0.05
	$R^2_{adj}$	0.999	0.998	0.996
	Reduced chi-square	0.04	0.49	1.72

efficiency variations as a function of PHAC dose at various initial 4CP concentrations (50–150 mg/L).

The adsorption efficiency of 4CP by PHAC was observed to improve gradually when the PHAC dose was increased from 0.5 to 2.5 g/L for all initially studied concentrations (50–150 mg/L). With the rising dose of PHAC from 0.5 to 2.5 g/L, the 4CP removal efficiency enhanced from 78.6 ± 3.9 to 100.0 ± 0.0%, from 73.4 ± 3.2 to 100.0 ± 0.0%, and from 66.9 ± 3.3 to 100.0 ± 0.0% at 50, 100, and 150 mg/L of 4CP concentration, respectively. When a higher dose of PHAC is used, the higher amount of surface and pore volume of the sorbent is available and providing greater active sites of sorption and more functional groups, and as a result, the higher 4CP adsorption efficiency is occurred (Li et al. 2003). Latip et al. (Badu Latip et al. 2020) evaluated the 2,4DCF adsorption from wastewater by Fe<sub>3</sub>O<sub>4</sub>@AC and showed that the removal efficiency of 2,4DCF enhanced upon the sorbent

dose ascending to 20 mg/L but reached constant removal efficiency on further increasing the sorbent dose.

### Effect of contact time

In order to realize the equilibrium time for maximum 4CP adsorption, the experiments of 4CP adsorption by PHAC were conducted as a function of contact time. Figure 11 presents the variation of 4CP removal under different 4CP concentrations (50–150 mg/L) by changing the contact time ranging from 2 to 120 min.

As shown in Fig. 11, the progress in contact time leads to improve the removal efficiency of 4CP. The instant 4CP removal was observed in the first part of the adsorption process (contact time lower than 20 min), which dropped gradually and attained equilibrium at around 60 min. More vacant sites on the sorbent surface area are available in the initial stage of

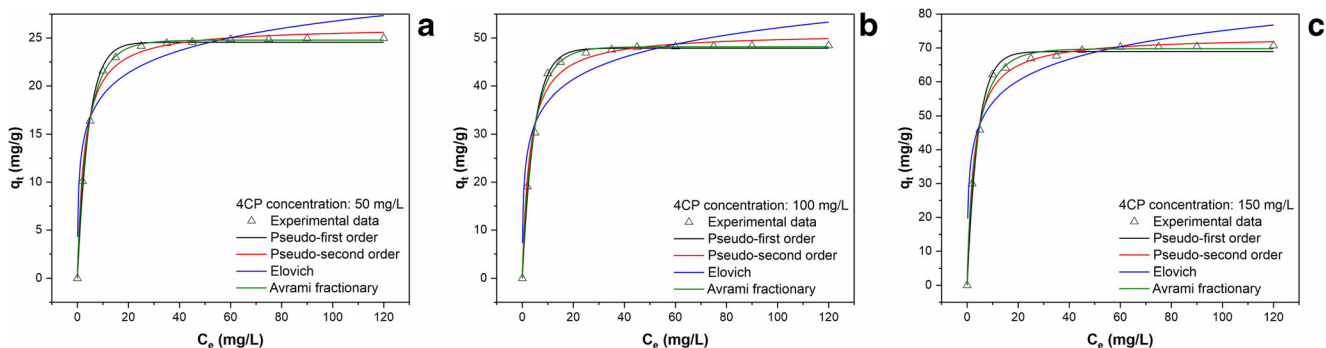


**Fig. 12** Plots of different kinetic models for 4CP adsorption onto PHAC (a) 50 mg/L of 4CP, (b) 100 mg/L of 4CP, and (c) 150 mg/L of 4CP



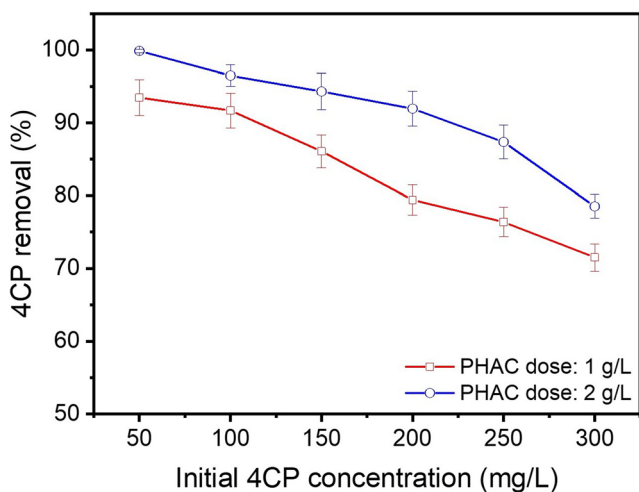


**Fig. 13** Variation of 4CP adsorption under different initial 4CP concentrations (PHAC dose, 200–600 mg/L; solution pH, 6; and contact time, 60 min)

the adsorption process and lead to an increasing gradient of concentration between adsorbate in bulk solution and sorbent surface, and as a result, the fast initial adsorption occurred. This behavior may be related to the strong, attractive forces between the active sorbent site and 4CP molecules and quick 4CP diffusion into the interparticle matrix to reach the rapid equilibrium (Sathishkumar et al. 2007). Further contact time increasing leads to declining the availability of active sites and uncovered surface area and decreasing the driving force. Consequently, the extended contact time is required to attain equilibrium for slowly diffusing of 4CP molecules into the sorbent intraparticle pores (Li et al. 2010). Besides, the curve of 4CP removal by PHAC as a function of contact time is single and continuous to achieve the saturation and indicating the monolayer coverage possibility of 4CP on the PHAC outer surface (Bilgili et al. 2012). Hameed et al. (2008) described that the higher initial 4CP concentration leads to a superior driving force and enables to overcome 4CP mass transfer boundary between bulk solution and sorbent surface.

**Kinetic study**

In order to realize the rate-controlling step and to determine the involved mechanisms and dynamics in 4CP adsorption,

**Table 4** Adsorption kinetic models and parameters

Isotherm model	Equation
Freundlich	$q_e = K_F C_f^{1/n_F}$ (9)
Langmuir	$q_e = Q_{max} K_L \frac{C_f}{1 + K_L C_f}$ (10)
Liu	$q_e = Q_{max} \left( K_g \frac{C_f^{n_L}}{1 + (K_g C_f)^{n_L}} \right)^{n_L}$ (11)

**Table 5** Values of isotherm parameters and correlation coefficients for the adsorption of 4CP

Isotherm model	Constant parameter	AC dose (g/L)	
		1.0	2.0
Freundlich	$K_F$	36.15 ± 3.62	39.79 ± 3.85
	$n_F$	2.48 ± 0.16	3.66 ± 0.04
	$R^2_{adj}$	0.992	0.979
	Reduced chi-square	4.96	4.02
Langmuir	$Q_{max}$	241.94 ± 14.72	128.34 ± 11.09
	$K_L$	0.062 ± 0.012	0.16 ± 0.05
	$R^2_{adj}$	0.983	0.950
	Reduced chi-square	10.16	9.06
Liu	$Q_{max}$	448.45 ± 20.9	273.73 ± 21.7
	$K_g$	0.0098 ± 0.001	0.0089 ± 0.001
	$n_L$	0.59 ± 0.13	0.39 ± 0.13
	$R^2_{adj}$	0.993	0.980
	Reduced chi-square	4.02	4.24

the kinetic models including pseudo-first order, pseudo-second order, Elovich, and Avrami fractional order (Eqs. (3–6)) were considered as summarized in Table 2.

where  $q_t$  reveals the sorption capacity at time  $t$  (mg/g),  $k_f$  and  $k_s$  are the rates constant of pseudo-first order ( $\text{min}^{-1}$ ) and pseudo-second order (g/mg.min), respectively,  $\alpha$  is the initial adsorption rate (g/mg.min),  $\beta$  is the activation energy and extent of surface coverage in chemisorption (g/mg), and  $k_{AV}$  and  $n_{AV}$  are Avrami kinetic constant ( $\text{min}^{-1}$ ) and fractional adsorption order, respectively.

The obtained experimental data on 4CP adsorption by PHAC with changing contact time were fitted with the kinetic models (Table 2) by using an Origin 8.5 software. The kinetic models' validity and their fitting quality were specified by calculating the determination coefficient ( $R^2$ ) and adjusted  $R^2$  ( $R^2_{adj}$ ) by Eqs. (7) and (8).

$$R^2 = \frac{\sum_i^{n_p} (q_{i,\text{exp}} - \bar{q}_{\text{exp}})^2 - \sum_i^{n_p} (q_{i,\text{exp}} - q_{i,\text{model}})^2}{\sum_i^{n_p} (q_{i,\text{exp}} - \bar{q}_{\text{exp}})^2} \tag{7}$$

$$R^2_{adj} = 1 - (1 - R^2) \left( \frac{n_p - 1}{n_p - p - 1} \right) \tag{8}$$

Figure 12 illustrated the obtained experimental data and predicted values of kinetic models, and estimated kinetic constants are summarized in Table 3.

The results revealed that, for the studied initial 4CP concentration, the  $R^2_{adj}$  value of Avrami fractional order was higher than other kinetic models, indicating more suitability of this kinetic model for 4CP adsorption prediction by PHAC as a function on contact time.

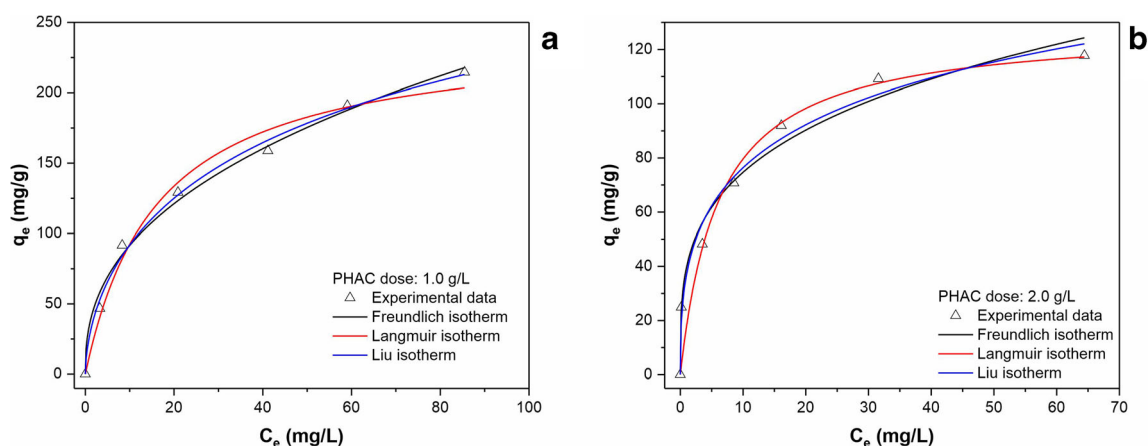


**Fig. 14** Plots of isotherm models for 4CP adsorption by AC: (a) 1 g/L of PHAC and (b) 2 g/L of PHAC

### Influence of initial concentration of 4CP

The obtained results related to the influence of the initial concentration of 4CP on the efficiency of 4CP adsorption at PHAC dose of 1 and 2 g/L are illustrated in Fig. 13.

As can be observed, in both doses of PHAC, with expanding initial 4CP concentration, the 4CP adsorption efficiency was declined. When 1 and 2 g/L of PHAC applied, with increasing initial concentration of 4CP ranging from 50.0 to 300.0 mg/L, the 4CP adsorption efficiencies were reduced from  $93.5 \pm 2.5$  to  $71.5 \pm 1.9\%$  and from  $99.8 \pm 0.2\%$ , respectively. This can be explained by the adsorption sites saturation of the adsorbent surface, which indicated a possible formation of a monolayer of 4CP molecules at the interface with the adsorbent (Yadav et al. 2020). The obtained results are in line with the presented results with Kilic et al. (2011), who reported that the adsorption efficiency of AC diminished with an increasing initial concentration of phenol.

### Isotherm study

The experiments of 4CP adsorption by PHAC were conducted in the batch mode system to obtain 4CP concentrations in the

bulk liquid phase. Several adsorption models can be used to describe experimental data of adsorption isotherms. According to Table 4, the equilibrium data were modeled with the Freundlich, Langmuir, and Liu isotherms (Eqs. (9–11)).

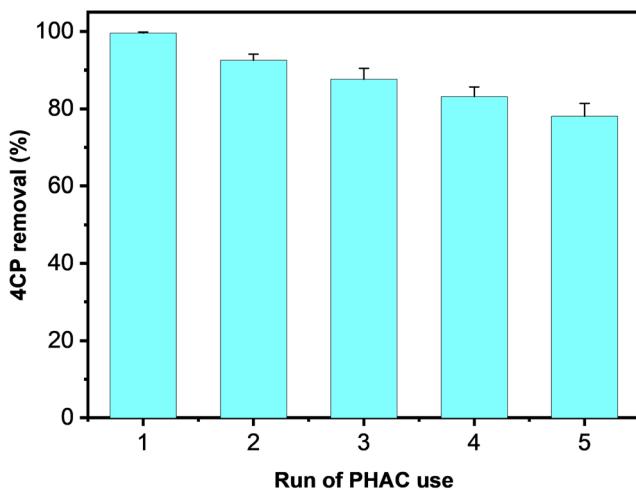
where  $n_F$  and  $K_F$  are Freundlich exponent and equilibrium constant (mg/g), respectively,  $K_L$  is the Langmuir equilibrium constant (L/mg),  $Q_{max}$  is the maximum sorption capacity (mg/g), and  $n_L$  and  $K_g$  are Liu exponent and equilibrium constant (L/mg), respectively.

Figure 14 shows the obtained fitting results of adsorption data at the studied dose of PHAC with different isotherm equations, and the obtained parameters were summarized in Table 5.

The results show that the higher  $R^2_{adj}$  related to Liu isotherm indicates that this model is more suitable than other isotherms for the prediction of 4CP adsorption by PHAC. As reported in Table 5, the theoretical values of  $Q_{max}$  of PHAC estimated by Liu isotherm at 1 and 2 g/L of PHAC dose were  $448.45 \pm 20.9$  and  $273.73 \pm 21.7$  mg/g, respectively. The comparison of the  $Q_{max}$  value of various AC is summarized in Table 6 and depicted that the obtained  $Q_{max}$  in present study is relatively higher than other studies.

**Table 6**  $Q_{max}$  value of some AC for 4CP adsorption

Raw material	Chemical activation agent	$Q_{max}$ (mg/g)	Refs.
Milk vetch	H <sub>3</sub> PO <sub>4</sub>	87	(Noorimotlagh et al. 2016)
Sewage sludge	KOH	192	(Monsalvo et al. 2012)
Jackfruit	H <sub>2</sub> SO <sub>4</sub>	277	(Jain and Jayaram 2007)
Sewage sludge	KOH	358	(Monsalvo et al. 2011)
Pistachio shells	NaOH	428	(Tseng et al. 2010)
Olive stones	H <sub>3</sub> PO <sub>4</sub>	436	(Termoul et al. 2006)
Corn cob	KOH	446	(Tseng and Tseng 2005)
Pomegranate husk	ZnCl <sub>2</sub> /NaOH	448	Present study



**Fig. 15** Reusability of PHAC for the removal of 4CP (4CP concentration, 50 mg/L; PHAC dose, 2.0 g/L; solution pH, 6.0; and contact time, 60 min)

### Reusability and stability

The reusability of the PHAC was assessed through five adsorption-desorption cycles. Each of the cycle was conducted at the optimum conditions (4CP concentration, 50 mg/L; PHAC dose, 2.0 g/L; solution pH, 6.0; and contact time, 60 min), and the desorption cycle was carried out using 5 mL of acetonitrile/methanol (1/1, v/v), vibrated under 180 rpm for 2 h at room temperature. The adsorbent was subsequently filtered and dried overnight for next use. The results regarding the 4CP removal efficiency for five cycles of PHAC are given in Fig. 15.

As illustrated in Fig. 15, the adsorption efficiency of 4CP was slightly declined after five consecutive cycles. The 4CP adsorption efficiency slightly reduced from 99.6% in the first cycle to 80% after the fifth run, indicating that as-prepared PHAC has a satisfactory reusability potential and can be recycled for several times with adsorption efficiency higher than 80%. These findings elucidate that the operation cost in practical applications could significantly be reduced due to the high operational reusability. However, the reason of this negligible reduction can be attributed to either minimal mass loss of PHAC during operation or reduction of the adsorption capacity of PHAC via blocking of the surface pores by 4CP.

### Conclusion

This study has dealt with the fabrication of AC from pomegranate husk by dual consecutive chemical activation. The effect of influencing parameters on the adsorption process such as solution pH, contact time, PHAC dose, initial concentration of 4CP, and adsorption temperature was assessed. The obtained data from batch adsorption experiments were

analyzed with different isotherms and kinetic models. Based on the obtained data, the following results can be concluded as:

- The present work is demonstrating that PHAC is capable of removing the 4CP from synthetic wastewater with high efficiency.
- Higher adsorption efficiency of 4CP was attainable in a higher dose of PHAC.
- The highest 4CP removal efficiency was obtained at solution pH ranging from 3 to 6.
- For all initial studied concentration of 4CP, the equilibrium between adsorbate in bulk solution and sorbent surface was attained at a contact time of lower than 60 min
- The optimum conditions of 4CP removal were initial 4CP concentration of 50 mg/L, solution pH of 6, PHAC dose of 2.5 g/L, and adsorption temperature of 313 K.
- The Liu isotherm and Avrami fractional order were the best models for representing the 4CP adsorption by PHAC with a good correlation.
- The adsorption efficiency of more than 80% was still obtained for 4CP after five consecutive cycles of adsorption.

**Authors' contributions** **Sousan Hadi:** Investigation, Data curation, Writing (original draft preparation); **Ensiyeh Taheri:** Investigation, Data curation, Formal analysis, Writing (original draft preparation); **Mohammad Mehdi Amin:** Data curation, Writing (original draft preparation); **Ali Fatehizadeh:** Conceptualization, Supervision, Methodology, Writing (original draft preparation); **Eder C. Lima:** Software, Writing (review and editing).

**Funding** The current research was supported by Isfahan University of Medical Sciences (Grant No. 298169 and ethical code #IR.MUI.RESEARCH.REC.1398.636). E.C. Lima thanks to CNPq (303.622/2017-2) and FAPERGS (19/2551-0001865-7).

### Compliance with ethical standards

**Competing interests** The authors declare no conflict of interest.

**Ethical approval** All procedures performed in this study were in accordance with the ethical standards of the Iranian national research committee and its later amendments or comparable ethical standards.

**Consent to participate** The manuscript is an original work of all authors and all authors made a significant contribution to this study.

**Consent to publish** The authors hereby consent to the publication of the work in Environmental Science and Pollution Research journal.

### References

- Al-Degs YS, El-Barghouthi MI, El-Sheikh AH, Walker GM (2008) Effect of solution pH, ionic strength, and temperature on adsorption behavior of reactive dyes on activated carbon. *Dyes Pigments* 77: 16–23

- Babu KS, Reddy AR, Sujatha C, Reddy KV, Mallika A (2013) Synthesis and optical characterization of porous ZnO. *J Adv Ceram* 2:260–265
- Badu Latip NM, Gopal K, Suwaibatu M, Hashim NM, Rahim NY, Raov M, Yahaya N, Mohamad Zain NN (2020) Removal of 2, 4-dichlorophenol from wastewater by an efficient adsorbent of magnetic activated carbon. *Sep Sci Technol* 1–14
- Bilgili MS (2006) Adsorption of 4-chlorophenol from aqueous solutions by xad-4 resin: isotherm, kinetic, and thermodynamic analysis. *J Hazard Mater* 137:157–164
- Bilgili MS, Varank G, Sekman E, Top S, Özçimen D (2012) Modeling 4-chlorophenol removal from aqueous solutions by granular activated carbon. *Environ Model Assess* 17:289–300
- Boudrahem F, Aissani-Benissad F, Ait-Amar H (2009) Batch sorption dynamics and equilibrium for the removal of lead ions from aqueous phase using activated carbon developed from coffee residue activated with zinc chloride. *J Environ Manag* 90:3031–3039
- Chen C, Wang X (2007) Influence of pH, soil humic/fulvic acid, ionic strength and foreign ions on sorption of thorium (IV) onto  $\gamma$ -Al<sub>2</sub>O<sub>3</sub>. *Appl Geochem* 22:436–445
- Fatehizadeh A, Zare MR, Van Ginkel SW, Taheri E, Amin MM, Rafiei N, Mahdavi M (2019) Methyl tertiary-butyl ether adsorption by bioactivated carbon from aqueous solution: kinetics, isotherm and artificial neural network modeling. *Desalin Water Treat* 154:254–267
- Gratis MKB, Panyathanmaporn T, Chumnanklang R-A, Sirinuntawittaya N, Dutta A (2008) Production of activated carbon from coconut shell: optimization using response surface methodology. *Bioresour Technol* 99:4887–4895
- Gupta V, Nayak A (2012) Cadmium removal and recovery from aqueous solutions by novel adsorbents prepared from orange peel and Fe<sub>2</sub>O<sub>3</sub> nanoparticles. *Chem Eng J* 180:81–90
- Hadi S, Taheri E, Amin MM, Fatehizadeh A, Aminabhavi TM (2020) Synergistic degradation of 4-chlorophenol by persulfate and oxalic acid mixture with heterogeneous Fenton like system for wastewater treatment: adaptive neuro-fuzzy inference systems modeling. *J Environ Manag* 268:110678
- Hameed B, Chin L, Rengaraj S (2008) Adsorption of 4-chlorophenol onto activated carbon prepared from rattan sawdust. *Desalination* 225:185–198
- Jain S, Jayaram RV (2007) Adsorption of phenol and substituted chlorophenols from aqueous solution by activated carbon prepared from jackfruit (*Artocarpus heterophyllus*) peel-kinetics and equilibrium studies. *Sep Sci Technol* 42:2019–2032
- Kilic M, Apaydin-Varol E, Pütün AE (2011) Adsorptive removal of phenol from aqueous solutions on activated carbon prepared from tobacco residues: equilibrium, kinetics and thermodynamics. *J Hazard Mater* 189:397–403
- Kosmulski M (2009) Surface charging and points of zero charge, vol 145. CRC Press
- Kuśmierk K, Świątkowski A, Kotkowski T, Cherbański R, Molga E (2020) Adsorption properties of activated tire pyrolysis chars for phenol and chlorophenols. *Chem Eng Technol* 43:770–780
- Latinwo GK, Alade AO, Agarry SE, Dada EO (2019) Optimization of process parameters for the production of activated carbon from *Delonix regia* pod through chemical activation and carbonization process applied. *J Environ Eng Sci* 5:2075–2098
- Li Y-H, Luan Z, Xiao X, Zhou X, Xu C, Wu D, Wei B (2003) Removal of Cu<sup>2+</sup> ions from aqueous solutions by carbon nanotubes. *Adsorpt Sci Technol* 21:475–485
- Li Y, Du Q, Wang X, Zhang P, Wang D, Wang Z, Xia Y (2010) Removal of lead from aqueous solution by activated carbon prepared from *Enteromorpha prolifera* by zinc chloride activation. *J Hazard Mater* 183:583–589
- Lima DR et al (2019) Efficient acetaminophen removal from water and hospital effluents treatment by activated carbons derived from Brazil nutshells. *Colloids Surf A Physicochem Eng Asp* 583:123966
- Maciá-Agulló J, Moore B, Cazorla-Amorós D, Linares-Solano A (2004) Activation of coal tar pitch carbon fibres: physical activation vs. chemical activation. *Carbon* 42:1367–1370
- Monsalvo VM, Mohedano AF, Rodriguez JJ (2011) Activated carbons from sewage sludge: application to aqueous-phase adsorption of 4-chlorophenol. *Desalination* 277:377–382
- Monsalvo VM, Mohedano AF, Rodriguez JJ (2012) Adsorption of 4-chlorophenol by inexpensive sewage sludge-based adsorbents. *Chem Eng Res Des* 90:1807–1814
- Noorimotlagh Z, Shahriyar S, Darvishi Cheshmeh Soltani R, Tajik R (2016) Optimized adsorption of 4-chlorophenol onto activated carbon derived from milk vetch utilizing response surface methodology. *Desalin Water Treat* 57:14213–14226
- Ribas MC, Adebayo MA, Prola LDT, Lima EC, Cataluña R, Feris LA, Puchana-Rosero MJ, Machado FM, Pavan FA, Calvete T (2014) Comparison of a homemade cocoa shell activated carbon with commercial activated carbon for the removal of reactive violet 5 dye from aqueous solutions. *Chem Eng J* 248:315–326
- Sajjadi S-A, Meknati A, Lima EC, Dotto GL, Mendoza-Castillo DI, Anastopoulos I, Alakhras F, Unuabonah EI, Singh P, Hosseini-Bandegharai A (2019) A novel route for preparation of chemically activated carbon from pistachio wood for highly efficient Pb (II) sorption. *J Environ Manag* 236:34–44
- Sathishkumar M, Binupriya AR, Vijayaraghavan K, Yun SI (2007) Two and three-parameter isothermal modeling for liquid-phase sorption of procion blue H-B by inactive mycelial biomass of *Panus fulvus*. *J Chem Technol Biotechnol* 82:389–398
- Shaarani F, Hameed B (2011) Ammonia-modified activated carbon for the adsorption of 2, 4-dichlorophenol. *Chem Eng J* 169:180–185
- Srivastava S, Tyagi R, Pal N, Mohan D (1997) Process development for removal of substituted phenol by carbonaceous adsorbent obtained from fertilizer waste. *J Environ Eng* 123:842–851
- Termoul M, Bestani B, Benderdouche N, Belhakem M, Naffrechoux E (2006) Removal of phenol and 4-chlorophenol from aqueous solutions by olive stone-based activated carbon. *Adsorpt Sci Technol* 24:375–388
- Tseng R-L, Tseng S-K (2005) Pore structure and adsorption performance of the KOH-activated carbons prepared from corncob. *J Colloid Interface Sci* 287:428–437
- Tseng R-L, Wu K-T, Wu F-C, Juang R-S (2010) Kinetic studies on the adsorption of phenol, 4-chlorophenol, and 2, 4-dichlorophenol from water using activated carbons. *J Environ Manag* 91:2208–2214
- Umpierrez CS, Thue PS, Lima EC, Reis GS, de Brum IAS, Alencar WS, Dias SLP, Dotto GL (2018) Microwave-activated carbons from tucumã (*Astrocaryum aculeatum*) seed for efficient removal of 2-nitrophenol from aqueous solutions. *Environ Technol* 39:1173–1187
- Wang L, Zhang J, Zhao R, Li Y, Li C, Zhang C (2010) Adsorption of Pb (II) on activated carbon prepared from *Polygonum orientale* Linn.: kinetics, isotherms, pH, and ionic strength studies. *Bioresour Technol* 101:5808–5814
- Wigmans T (1989) Industrial aspects of production and use of activated carbons. *Carbon* 27:13–22
- Yadav S, Asthana A, Chakraborty R, Jain B, Singh AK, Carabineiro SAC, Susan MABH (2020) Cationic dye removal using novel magnetic/activated charcoal/ $\beta$ -cyclodextrin/alginate polymer nanocomposite. *Nanomaterials* 10:170

**Publisher's note** Springer Nature remains neutral with regard to jurisdictional claims in published maps and institutional affiliations.